Integrability and localized excitations in nonlinear discrete systems

S. Flach* and C. R. Willis
Department of Physics, Boston University, 590 Commonwealth Avenue, Boston, Massachusetts 02215

E. Olbrich
Institut für Theoretische Physik, Technische Universität Dresden, 01062 Dresden, Federal Republic of Germany
(Received 12 August 1993)

We analyze the origin and features of localized excitations in nonlinear discrete Klein-Gordon systems. We connect the presence of stationary excitations with the existence of local integrability of the original N-degree-of-freedom system. The method consists of constructing a reduced problem of a few degrees of freedom and analyzing its phase-space structure with the help of geometrical methods (Poincaré maps). We find a correspondence between regular and chaotic motion in the reduced problem on one side and localized and delocalized states in the infinite system on the other side. The periodic trajectories corresponding to elliptic fixed points of the Poincaré map are related to previous numerical and analytical studies. We analyze the stability of the periodic orbits with respect to small-amplitude phonons as well as the internal stability of multiple-frequency localized excitations. We find an energy threshold for the existence of stationary localized excitations and an energy threshold for the existence of instabilities due to internal resonances (onset of chaos). Approximation schemes accounting for the main properties of stationary localized excitations are applied.

PACS number(s): 03.20.+i, 63.20.Pw, 63.20.Ry

I. INTRODUCTION

In this paper we study nonlinear localized excitations (NLEs) in various Hamiltonian lattices of the nonlinear Klein-Gordon type. There are several reasons for studying NLEs. First there is the general problem of localization phenomena in systems with *and without* disorder. Second we mention the links between regular and stochastic motion on one side and dynamic properties of complex systems with many degrees of freedom on the other side. Finally the connection between continuum systems (partial differential equations) and discrete systems (coupled ordinary differential equations) still possesses many unresolved puzzles in the description of nonlinear phenomena.

Localization phenomena in partial differential equations (PDEs) are usually projected onto properties of soliton and solitary solutions and are widely studied [1]. Much less is known about localization properties in coupled ordinary differential equations (CODE). This is especially true for localized excitations with internal oscillating degrees of freedom such as the breather modes in the continuum sine-Gordon system [2]. The reason for that is the loss of the continuous translational symmetry going over from PDE to CODE. The remaining discrete translational symmetry in CODE is too weak to be useful for the study of dynamic solutions. Thus it was natural to study first the subclass of integrable CODE, since the presence of additional global constants of motion suggests the existence of hidden additional symmetries. Using the powerful inverse scattering technique Ablowitz and Ladik found an integrable lattice model, which possesses localized excitations with an internal oscillating degree of freedom (in analogy to continuum sine-Gordon breathers) [3]. However, to proceed in the understanding of the matter of interest it is necessary to study nonintegrable CODE.

Several attempts to do so are known. The most intensive studies were done by Takeno, Sievers, Hori, and co-workers (see [4–7] and references therein) and Page *et al.* [8, 9] (it is impossible to cite all contributions to this subject; for more recent developments see [10]). The object of their study was the famous Fermi-Pasta-Ulam (FPU) system (see, e.g., [11]). These one-dimensional chains are characterized by particles connected with their nearest neighbors via nonlinear springs, where the spring potential is a certain polynomial of nth degree in the relative coordinates of two nearest neighbors. These systems have at least two global constants of motion—total energy and momentum. In a certain continuum limit the FPU system can be mapped onto a special PDE, namely, the Korteweg–deVries equation [12], which is completely integrable, but possesses *no breathers*. So it came as a surprise that Takeno *et al.* found rather stable long-lived breatherlike excitations on the FPU lattice, which could even move over long distances through the lattice. Together with the fact that the frequencies of those nonlinear localized excitations were well *above* the phonon band (of small amplitude oscillations near the ground state), it was logical to assume that those NLEs are not connected to similar excitations of the corresponding PDE. Indeed making the continuum limit, i.e., going over from a CODE to a corresponding PDE, one is left with a phonon band, where the upper band edge is shifted to infinity. Thus the NLE frequencies also shift to infinity and become meaningless in the continuum limit. How-

*Electronic address: flach@buphy.bu.edu

ever, this kind of argument is essentially based on the proper choice of energy scales of the CODE in the continuum limit. In other words, if one chooses an energy scale where the dispersion relation between the frequency and wave number of small amplitude phonons is linear, the above statement about the continuum limit is true. As we will show in Sec. II, the proper choice of an energy scale is as essential in nonlinear systems as the choice of several model parameters. For example, it was shown [5] that the NLE solution in the discrete FPU lattice becomes nearly delocalized if the frequency of the NLE is lowered to the upper phonon band edge. Thus we have a solution on the lattice, which can be described by a field (slow spatial variations), although the frequency of the field's oscillation is slightly *above* the upper phonon band edge (cf. [13]). As long as one considers this particular weakly localized NLE solution, one could replace the CODE by a proper PDE.

The existence of total momentum conservation law in the FPU systems is directly linked to the absence of a phonon gap. The phonon branch is acousticlike and the lower band edge frequency is zero. Breaking the momentum conservation would lead to a finite phonon gap and thus to a possibility of exciting NLEs with frequencies *below* the phonon band. In that case there is no principal hurdle to link NLEs of the CODE with solutions of the corresponding PDE. Adding so-called on-site potentials to the FPU Hamiltonian one indeed breaks the momentum conservation and lands in another important class of CODE, the discrete Klein-Gordon systems. Usually one reduces the spring potential to a harmonic one and adds the *necessary* nonlinearity into the on-site potentials. First the existence of NLEs with frequencies in the phonon gap was reported in [14] for a discrete Φ^4 system with single-well on-site potentials; later Campbell and Peyrard found breatherlike NLEs with frequencies in the phonon gap in the discrete Φ^4 system with double-well on-site potentials [15]. The existence of the same type of NLEs was confirmed also for a Φ^3 system [16].

Recently two of us have shown that the properties of NLEs in discrete Klein-Gordon systems are much richer than initially anticipated [17,18]. Especially we were able to describe the properties of NLEs in a reduced problem of a few degrees of freedom. We linked the existence of regular motion of the reduced problem on a torus to the existence of *multiple frequency stationary* NLEs in the infinite degree of freedom system. In this contribution we want to present a careful analysis of the correspondence between the reduced and the full problem. Our goal is to investigate the phase-space structure of the reduced problem and to show the linkage between regular and stochastic motion in the reduced problem on one side and localization properties of the full system on the other side.

The paper is organized as follows. In Sec. II we introduce the models and briefly characterize the main dynamic properties of NLEs. In Sec. III we discuss several numerical and analytical methods for obtaining such NLE solutions. In Sec. IV the reduced problem is introduced. We investigate the Poincaré map of the reduced problem over a large energy range. Then we show the correspondence between the reduced and full problems. Stability analysis of the NLEs is applied to relaxational and existence properties of NLEs in Sec. V. In Sec. VI we briefly review application of our method to several Klein-Gordon lattices. Section VII is used to sum up and discuss the results.

II. MODELS AND LOCALIZED SOLUTIONS

We study a class of $d = 1$ dimensional discrete classical models given by the Hamiltonian

$$H = \sum_{l=1}^{N} \left[\frac{1}{2} P_l^2 + \frac{1}{2} C (Q_l - Q_{l-1})^2 + V(Q_l) \right] . \quad (1)$$

P_l and Q_l are canonically conjugated momentum and displacement of the lth particle, where l marks the number of the unit cell. C measures the interaction to the nearest-neighbor particles. All variables are dimensionless. The mass of the particles is equal to unity. N is the total number of particles. The nonlinearity appears in the on-site potential $V(x)$. Typical examples of $V(x)$ are (i) Φ^3,

$$V(x) = V_{\Phi^3}(x) = \frac{1}{2} x^2 - \frac{1}{3} x^3 , \quad (2)$$

(ii) Φ^4,

$$V(x) = V_{\Phi^4}(x) = \frac{1}{4} (x^2 - 1)^2 , \quad (3)$$

and (iii) *double quadratic* (DQ),

$$V(x) = V_{\mathrm{DQ}}(x) = \frac{1}{2} (|x| - 1)^2 . \quad (4)$$

Examples (ii) and (iii) are multiwell potentials leading to two degenerated ground states of the Hamiltonian (1). The Φ^3 case gives one local ground state, separated by a barrier from a global instability. The important difference between DQ on one side and Φ^4 and Φ^3 on the other side is that the whole nonlinearity of the DQ potential appears in the point $x = 0$.

To produce nonlinear localized excitations numerically (if the system allows for their existence) we choose an initial condition which corresponds to a localization of energy. In [17] we simply positioned the whole system into its ground state and then displaced one (central) particle by a given amount of displacement. Then the evolution of the system can be studied by means of molecular dynamics. We used always periodic boundary conditions. Since some amount of the initial energy will be transformed into traveling phonons (radiation), one has to take care of the system size to exclude effects of return. This can be done in two ways: (i) by choosing a large enough system (thus making the time of return large) and/or (ii) by applying an additional friction to particles far away from the initial energy burst. We avoided (ii) since usually there will be some effects of phonon reflection at the boundary between the frictioned and nonfrictioned parts of the chain. We used the Verlet algorithm for solving the Newtonian equations of motion. The time step if not

indicated specially was $h = 0.005$. The system sizes were $N = 3000$ if not indicated specially.

Before coming to examples of NLE, let us mention the properties of (1) for small amplitude oscillations around the ground state. A simple calculation yields the following dispersion law for small-amplitude phonons:

$$\omega_q^2 = \omega_0^2 + 4C\sin^2(\pi q/N)\,, \tag{5}$$

where $q = 0, 1, 2, \ldots, (N-1)$ is the wave number, ω_q is the frequency of a phonon with wave vector q, and ω_0 measures the lower phonon band edge: $\omega_0 = 1$ for DQ and Φ^3 and $\omega_0 = \sqrt{2}$ for Φ^4.

Now let us show some typical examples of NLE for Φ^4 for a special choice of the interaction strength $C = 0.1$. This value was considered because it corresponds to a balance between the on-site energy of a particle and the energy of the springs connecting it to the neighbors for energies of the order of the barrier height of $V(x)$. Usually it is argued that (1) and (3) have a displacive limit $C \geq 1$ and an order-disorder limit $C \ll 1$ [19]. However, because of the nonlinearity we have a second parameter—the energy. Thus what one has to do is to study the behavior of the system in the phase plane {energy,C}. Since we are looking for localized excitations, we do so by calculating the on-site potential energy of one displaced particle and the spring (interaction) energy, if all other particles are holded at their ground state position η (e.g., $\eta = -1$). The result is shown in Fig. 1 where the different parts of the energy are plotted versus amplitude of the displaced particle for several interaction strengths C. We see that for $C \geq 1$ for all amplitudes smaller than a certain C-dependent threshold the system is displacive, i.e., the energy of the springs overcomes the on-site energy. Above that threshold the system becomes closer to uncorrelated particles. That C interval could be defined as the displacive or better strongly correlated limit.

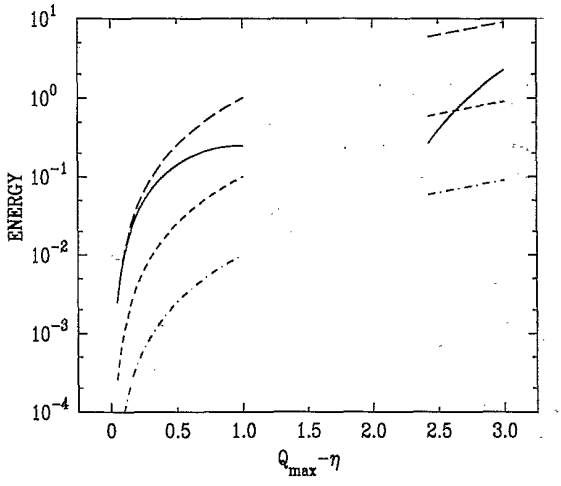

FIG. 1. Potential energy versus initial displacement $Q_{\max}$ for a particle in a Φ^4 chain, where all other particles are fixed at the ground state position $\eta = -1$. Solid line, on-site energy (3); long dashed line, spring energy for $C = 1$; short dashed line, spring energy for $C = 0.1$; dash-dotted line, spring energy for $C = 0.01$. Note the discontinuity because of the barrier in (3).

For $0.05 < C < 1$ we find two amplitude thresholds: if the amplitude is lower than the smaller threshold or larger than the larger threshold we have weak interactions, whereas in between the two threshold values the choosen amplitude yields slightly stronger interaction energies than on-site energies. In that sense this C interval can be defined as an intermediate coupling. For $C \leq 0.05$ the interaction energy is always small compared to the on-site energy. Thus we can call this C interval as a weak correlated limit. From the above it becomes clear that the choosen value of $C = 0.1$ and energy ranges around 0.25 certainly cannot be addressed to weak correlations, since the coupling energy is of the same order as (and even slightly larger than) the on-site energy.

To characterize the behavior of the system we introduce a local energy variable e_l:

$$e_l = \frac{1}{2}P_l^2 + V(Q_l) + \frac{1}{4}C\left[(Q_l - Q_{l-1})^2 + (Q_l - Q_{l+1})^2\right]. \tag{6}$$

The sum over all local energies gives the total conserved energy. If NLE are excited, the initial local energy burst should mainly stay within the NLE. Thus defining

$$e_{(2m+1)} = \sum_{l=-m}^{m} e_l \tag{7}$$

and exciting the local energy burst at lattice site $l = 0$ by choosing a proper value of m in (6) we will control the time dependence of $e_{(2m+1)}$. If this function does not decay (or decay slowly enough) to zero, the existence of a NLE can be confirmed. The terminus "slowly enough" has to be specified with respect to the typical group velocities of small-amplitude phonons. This sets the time scale we are interested in

$$t \gg m\frac{\sqrt{\omega_0^2 + 2C}}{2C}\,. \tag{8}$$

In Fig. 2 we show the time dependence of $e_{(5)}$ for an ini-

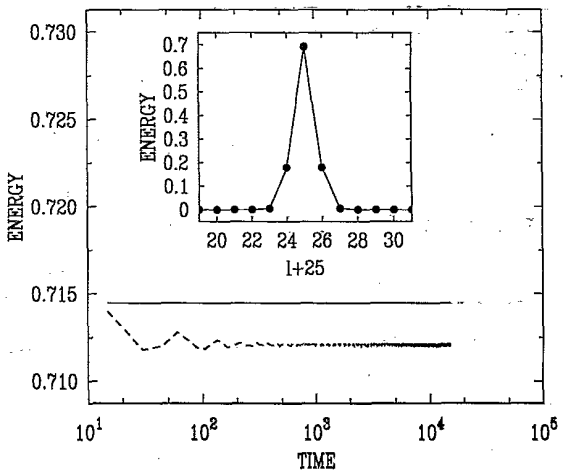

FIG. 2. $e_{(5)}$ versus time (dashed line) for Φ^4 with $C = 0.1$, $N = 3000$, and $Q_0(t = 0) = 1.3456$. Total energy of the chain, solid line. Inset: energy distribution $e_l^{\max}$ versus particle number for the same solution as in Fig. 2 measured for $1000 < t < 1150$.

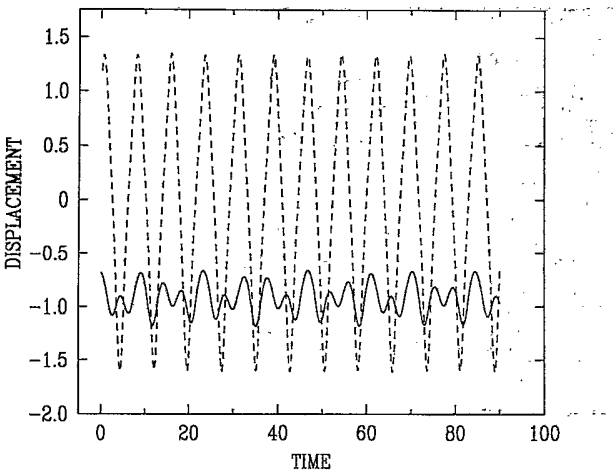

FIG. 3. Displacement of central particle (dashed line) and nearest-neighbor particles (solid line) versus time for the same initial condition as in Fig. 2. Note that measurement is performed after a waiting period of $t = 1000$.

tial condition $Q_0(t=0) = 1.3456$, $Q_{l\neq 0} = -1$, $\dot{Q}_l = 0$ of the Φ^4 system. Clearly a NLE is found. After a short time period of the order of 100 time units nearly constant values of $e_{(5)}$ are observed. The NLE is stable over a long period of time with some weak indication of energy radiation. The energy distribution within the NLE is shown in the inset of Fig. 2. Essentially three particles are involved in the motion, so we find a rather localized solution. In Fig. 3 we show the $Q_l(t)$ dependence for the central $l = 0$ and the nearest neighbors $l = \pm 1$ particles. While the central particle performs large-amplitude oscillations crossing the barrier of its on-site potential, the nearest neighbors are confined to the well of the chosen ground state.

Before characterizing the NLE more precisely, we will discuss in Sec. III known methods of approximate analytic handling of these objects, especially the rotating-wave approximation (RWA). We will show that the RWA can be a rather powerful method; however, it does not provide us with much physical insight into the origin of NLEs. Moreover we will see that the complexity of the problem can make the RWA useless in a practical sense, thus forcing us to understand and to describe the NLE in another way.

III. ROTATING-WAVE APPROXIMATION

A large number of publications originating in works of Takeno, Sievers, and Hori [4–6] view the NLE as monochromatic modes of the lattice, i.e., the solution is sought in the form

$$Q_l(t) = F_l(t) \,, \tag{9}$$

where the function $F_l(t)$ is periodic with some fundamental frequency ω_1:

$$F_l(t) = F_l(t+T_1) \,, \quad T_1 = \frac{2\pi}{\omega_1} \,. \tag{10}$$

This ansatz is motivated by the structure of the known solutions of breathers in some continuum models, which are the most prominent examples of localized vibrations in the continuum. The main idea of the RWA is to represent $F_l(t)$ in a Fourier series

$$F_l(t) = \sum_{k=-\infty}^{+\infty} \Phi_{lk} e^{ik\omega_1 t} \,, \tag{11}$$

to insert the ansatz into the original equations of motion, to collect terms with equal harmonics $k\omega_1$, $k = 0, \pm 1, \pm 2, \ldots$, and to neglect all coefficients in the Fourier representation of $F_l(t)$: $\Phi_{lk} = 0$ for $|k| \geq k_0$. The simplest version implies $k_0 = 2$, i.e., $F_l(t)$ is assumed to be a harmonic function. Before turning to the interacting case of many particles, let us shortly discuss the results of such an approach for the nonlinear motion of a single particle.

A. Single particle

We want to apply the RWA to the one-particle problem

$$\ddot{Q} = -V'(Q). \tag{12}$$

The potential $V(Q)$ should provide bound motion, at least for the cases under consideration. Since this problem is integrable, one can (at least numerically) calculate the period of the periodic solution (12) and thus the fundamental frequency. For example, for the class of potentials

$$V(Q) = \frac{1}{2m} Q^{2m} \tag{13}$$

the solution for the frequency can be found analytically as a function of the energy E:

$$\omega = \frac{1}{2}\sqrt{2\pi}(2m)^{1-1/2m} \frac{\Gamma(1/2m + 1/2)}{\Gamma(1/2m)} E^{1/2-1/2m} \,. \tag{14}$$

Here $\Gamma(x)$ is the gamma function. Applying RWA with $k_0 = 2$ one derives the approximation

$$\omega_1 = 2^{1-m}(2m)^{1/2-1/2m} \sqrt{\frac{(2m-1)!}{m!(m-1)!}} E^{1/2-1/2m} \,. \tag{15}$$

First we note the remarkable coincidence between the exact result (14) and the approximation (15) with respect to the energy dependence, which was achieved within the RWA using the exact relation between the amplitude and the energy as it follows from (13). Moreover comparing the prefactors for, e.g., $m = 2$ in (13) yields 1.1981 and 1.2247 for the exact result (14) and the approximation (15), respectively. That means that the simplest RWA in the case of (13) already gives an error of less then 2.3%.

Next we consider the Φ^4 potential (3). There it is known that the $\omega(E)$ dependence yields a minimum with $\omega = 0$ for $E = 0.25$ (the barrier height) [20, 21] [see the solid line in Fig. 4(a)]. To apply RWA in this case we

explicitly write down the resulting equations of the procedure as described at the beginning of Sec. III choosing $k_0 = 4$:

$$0 = -\Phi_0 + \Phi_0^3 + 6\Phi_0(\Phi_1^2 + \Phi_2^2 + \Phi_3^2) + 12\Phi_1\Phi_2\Phi_3 + 6\Phi_1^2\Phi_2 , \quad (16)$$

$$-\omega_1^2\Phi_1 = \Phi_1 - (3\Phi_0^2\Phi_1 + 6\Phi_0\Phi_1\Phi_2 + 3\Phi_1^3 + 6\Phi_1\Phi_2^2 + 6\Phi_0\Phi_2\Phi_3 + 3\Phi_1^2\Phi_3 + 6\Phi_1\Phi_3^2) , \quad (17)$$

$$-4\omega_1^2\Phi_2 = \Phi_2 - (3\Phi_0^2\Phi_2 + 3\Phi_0\Phi_1^2 + 6\Phi_1^2\Phi^2 + 3\Phi_2^3 + 6\Phi_0\Phi_1\Phi_3 + 6\Phi_1\Phi_2\Phi_3 + 6\Phi_2\Phi_3^2) , \quad (18)$$

$$-9\omega_1^2\Phi_3 = \Phi_3 - (3\Phi_0^2\Phi_3 + 3\Phi_3^3 + 6\Phi_0\Phi_1\Phi_2 + \Phi_1^3 + 6\Phi_1^2\Phi_3 + 6\Phi_2^2\Phi_3^3) . \quad (19)$$

Here we have used the time reversal symmetry of the exact solution of (12), i.e., by proper choosing of the time origin we have $\Phi_k = \Phi_{-k}$. To match the solutions onto a frequency-versus-energy dependence we use the exact relation between the amplitude of the motion and the energy for energies larger than the barrier height and the exact (numerically) relation between the mean position of the particle Φ_0 and the energy for energies below the barrier height. In the simplest approximation we again assume $k_0 = 2$. The corresponding RWA solution is shown in Fig. 4(a) (dashed line) and Fig. 4(b) (triangles). As it has to be expected, the approximate result is close to the exact line for small energies (nearly harmonic motion) and high energies (nearly quartic oscillator; cf. previous example). Significant deviations occur for energies around the barrier height, where the slowing down of the motion appears, thus higher terms in the RWA have to be taken into account. This is done for energies below the barrier height with $k_0 = 3$ [filled circles in Fig. 4(b)] and energies above the barrier height with $k_0 = 4$ [filled circles in Fig. 4(a)]. Note that due to the symmetry of the underlying potential $V(x) = V(-x)$ all even Fourier components Φ_{2m} vanish for energies above the barrier height. As a result of the increased number of components taken into account we clearly find a rather good agreement between RWA and the exact result. Thus the initial idea of the RWA seems to be fruitful—it should be enough to restrict the calculation onto a finite number of Fourier components in order to achieve quite reasonable results. However, there are two technical disadvantages of RWA already at this stage: in order to achieve the above results, we had to solve nonlinear sets of equations with already three variables, and we needed some input information, which was quite as complicated to calculate as the whole exact result. Nevertheless the success of RWA at this level is quite impressive. Let us step now to the more complex problem of interacting particles.

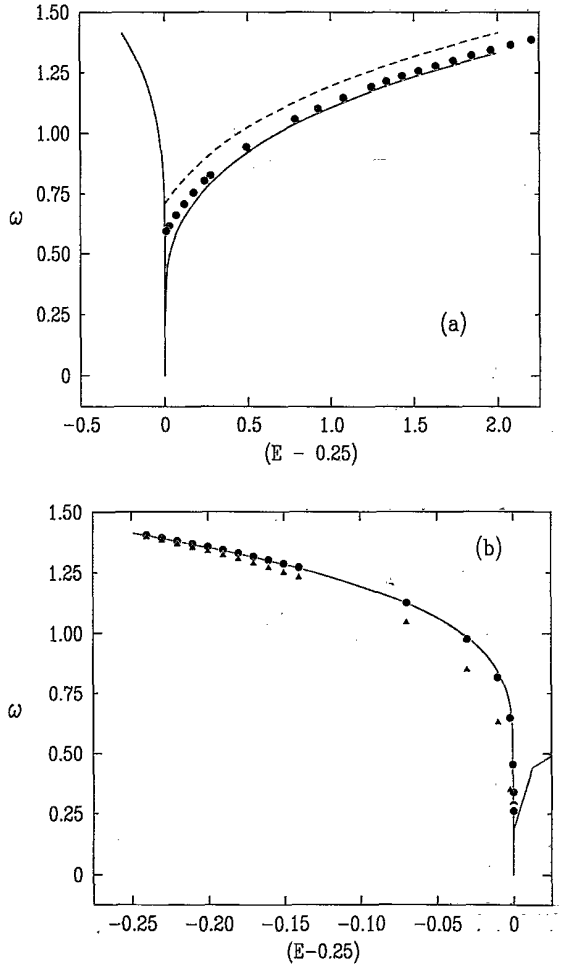

FIG. 4. Fundamental frequency ω versus energy for a particle motion in potential (3). (a) Solid line, exact result; dashed line, RWA $k_0 = 2$; filled circles, RWA $k_0 = 4$. (b) Solid line, exact result; triangles, RWA $k_0 = 2$; circles, RWA $k_0 = 3$.

B. Interacting particles

Taking into account the interaction does not complicate the RWA equations essentially. In fact every variable Φ in (16)–(19) carries now a second label of the lattice cite number, and due to the interaction terms with the structure

$$C(2\Phi_{lm} - \Phi_{(l-1)m} - \Phi_{(l+1)m}) \quad (20)$$

appear on the right hand side of these equations. The essential complication is the increasing number of variables and equations one has to solve. For example, assuming $k_0 = 3$ leads to six coupled equations for seven variables in the case of the NLE solution as described at the end of Sec. II and shown in Figs. 2 and and 3. Even one external condition leaves us with the problem to solve a set of equations with six variables. That is a rather difficult numerical task, not at least because these equations produce a huge number of solutions, and one has to decide which one to select. Of course, one can use iteration procedures [6], but since the structure of the equations is not very simple, the meaning of such procedures is difficult to understand.

There exist also other numerical methods to obtain periodic localized solutions on a lattice. Especially we

want to mention the results of Campbell and Peyrard [15]. They replaced the continuous time variable by a set of discrete time points (as usually done in every molecular dynamics simulation) and transformed the periodicity of the original solution in the continuous time variable into a periodicity on the discrete time grid. Then the equations of motion were rewritten in terms of a high dimensional Hamiltonian (phase-space volume preserving) iterated map. Finally periodic NLE solutions for Φ^4 systems were found starting with a nearby solution (from a continuum asymptotic expansion) and using a generalized Newton's iterative method. This method is also rather complicated and as in the RWA case (because of the nonlinearity of the problem) one needs an ansatz close enough to the wanted result.

To finish this section, we show a Fourier transformation of the motion of the central particle in the NLE as found in Fig. 2 [17]. The result is shown in Fig. 5. We see clearly that there are two frequencies determining the motion of the central particle $\omega_1 = 0.822$ and $\omega_2 = 1.34$. All peak positions in Fig. 5 can be explained through linear combinations of these two frequencies. To save the RWA, we now have to include the second frequency into the ansatz. This makes the number of variables again higher. Still we have no physical motivation for the new ansatz. Thus we feel we have no other choice than to give up the RWA concept and look for alternative ways of analysis. As it will be shown in the next section, a fruitful way is to follow methods of geometrical descriptions of classical mechanics.

IV. THE INTEGRABILITY CONCEPT

A. Basic ideas

From the last paragraph in Sec. III (see also [17]) we found the surprising result that the NLE might be described by two frequencies rather than by one. What can be the mathematical reason for that? To proceed

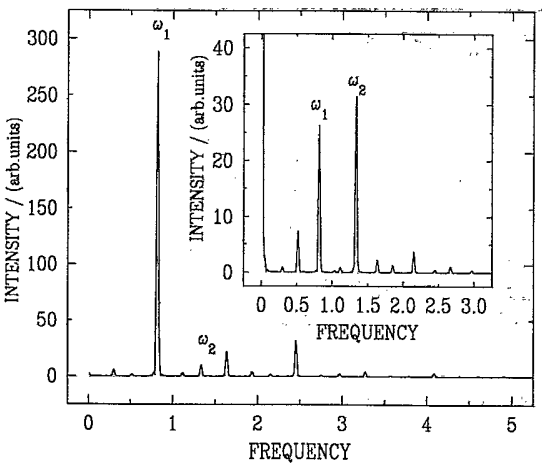

FIG. 5. Fourier transformed $\mathcal{T}_F[Q_l(t \geq 1000)](\omega)$ for Φ^4, $C = 0.1$, $N = 3000$, and the same initial conditions as in Fig. 2 with $l = 0$ (central particle). Inset: the same with $l = \pm 1$ (nearest neighbors).

in the understanding of the phenomenon, we plot in the inset in Fig. 5 the Fourier transformation of the motion of the nearest neighbor(s) to the central particle. As expected, we not only observe the two-frequency spectrum, but surprisingly the peak with the highest intensity is not at ω_1 as for the central particle, but at ω_2. It looks like every particle has its major frequency. Because of the symmetry of the initial condition the two nearest neighbors move in phase. Thus we are left with an effective two-degree-of-freedom problem (cf. inset in Fig.2).

Now it is a small step to recognize that we might be confronted with a kind of integrability phenomenon. Indeed, fixing the rest of the particles at their ground state positions reduces the dynamical problem to a two degree of freedom system, which might be integrable in parts of its phase space:

$$\ddot{Q}_0 = -V'_{\Phi^4}(Q_0) - 2C(Q_0 - Q_{\pm 1}) \ , \tag{21}$$

$$\ddot{Q}_{\pm 1} = -V'_{\Phi^4}(Q_{\pm 1}) - C(2Q_{\pm 1} - Q_0 + 1) \ . \tag{22}$$

We will call these types of few-degree-of-freedom systems *reduced problems*. As we have shown [17], the integrablity conjecture is indeed true. We performed a Poincaré intersection between the trajectory and the subspace $\{\dot{Q}_0, Q_0, Q_{\pm 1} = -1, \dot{Q}_{\pm 1} > 0\}$. Not only did we find the existence of regular motion on a two-dimensional torus, we also found nearly identical tori intersections for the reduced and full problems [17]. Thus we arrive at two conclusions: (i) the NLE existence is a result of (at least local) integrability properties of the underlying many-particle system; (ii) the NLE can be reproduced within a reduced problem, where all particles performing small-amplitude oscillations are fixed at their ground state positions, thereby reducing the number of relevant degrees of freedom.

With the integrability property in mind, it is clear that there have to appear two frequencies. If the reduced problem is integrable (in some part of phase space), there should appear two actions I_n, $n = 1, 2$, as functions of the original variables, so that the Hamiltonian of the reduced problem can be expressed through the two action variables only, and these actions become integrals of motion. The corresponding two frequencies

$$\omega_n = \frac{\partial H}{\partial I_n} \tag{23}$$

determine the motion of system on the surface of the torus. Obviously all linear combinations of multiples of these frequencies appear in the Fourier spectrum of the original particle displacements. That is exactly what we observe. The conclusions from above imply another consequence, namely, that an assymetric NLE (with respect to the central particle) should be possible too, i.e., that the two nearest neighbors perform not-in-phase motions, even with different amplitudes. That would mean that, in the language of actions, we lift a degeneracy by choosing asymmetric initial conditions and have to expect three, instead of two, fundamental frequencies, i.e., the frequency ω_2 splits into two frequencies $\omega_2 \neq \omega_3$. To check this statement we performed a simulation with an asymmetric initial condition, which differs from the pre-

vious symmetric initial condition by additionally choosing $Q_1(t=0) \neq \eta$. Indeed we found that (i) the local asymmetry is conserved throughout the evolution of the system, and (ii) as the Fourier spectrum of the central particle motion and the two nearest-neighbors motions show, we now find three frequencies: $\omega_1 = 0.83$, $\omega_2 = 1.32$, and $\omega_3 = 1.35$ [17].

Let us summarize the results up to now: the NLEs correspond to (nearly) regular trajectories in the phase space of the system under investigation; essentially a few degrees of freedom are excited; the trajectory (solution) is very close to a trajectory (under same initial conditions) of a reduced problem, reflecting the fact of localization *and* the excitation of only a few degrees of freedom.

B. The correspondence conjecture

To proceed in the description of the NLEs, we study the properties of the reduced problem more carefully. For that we first perform a Poincaré mapping for the entire available phase space of the reduced problem fixing the energy (for details about methods in nonlinear dynamics see [22]). The result is shown in Fig. 6. We observe several isolated regular islands embedded in a sea of chaotic trajectories. Our NLE, as described in Sec. IV A, corresponds to torus intersection in island 2. There is evidence that all regular solutions from island 2 correspond to NLE solutions in the full problem. All trajectories from island 2 have the property $|Q_0 - \eta|^{\max} \gg |Q_{\pm 1} - \eta|^{\max}$. This amplitude ratio is an indication that a solution of the reduced problem is close to a corresponding NLE solution of the full problem. We demonstrate our finding in Fig. 7, where we plot $e_{(5)}$ versus energy for two initial conditions in the infinite system which correspond to two trajectories from island 2—including the fixed point trajectory (point in island 2). Now we come close to an interesting result, namely, the existence of periodic localized solutions. These trajectories correspond to elliptic fixed points in Poincaré maps of the reduced problem. Thus the solutions of numerical methods such as RWA (cf. Sec. III) could yield exactly those fixed point solutions. However, we observe a much richer structure of multiple frequency NLEs which are smoothly connected to the fixed point solution.

Let us turn our interest to island 1 in Fig. 6. Again the amplitude ratio of the solutions from this island indicate that those solutions survive as NLEs in the full system. That this is indeed so, we show in Fig. 7 for two trajectories from island 1—the larger torus and the fixed point solution. Thus we arrive at the fact, that our geometrical method of studying Poincaré maps enables us to *predict and find* NLE solutions of the full system. Indeed the RWA or even the method used by Campbell and Peyrard (cf. Sec. III) can be now specified to be useful for calculating certain fixed point solutions. The necessary ingredient for those methods is *the symmetry* of the fixed points; in other words, one has to be close enough to a certain fixed point. To explain this point in more detail, we plot in Figs. 8(a) and 8(b) the $Q_l(t)$ dependence for the central $l = 0$ and the nearest-neighbor $l = \pm 1$ particles in the full system, using the fixed point solutions from islands 1 and 2 of the reduced problem as initial conditions, respectively. The fixed point solution from island 1 is characterized by in-phase motion of the central and nearest-neighbor particles, i.e., maxima and minima of the elongations for both particles appear at the same time [Fig. 8(a)]. For the fixed point solution from island 2 we find nearly period doubling for the central particle motion compared to the nearest-neighbor particle motion. However, still both elongations are periodic with the same time period [Fig. 8(b)].

What kind of trajectories do we find in island 3? The

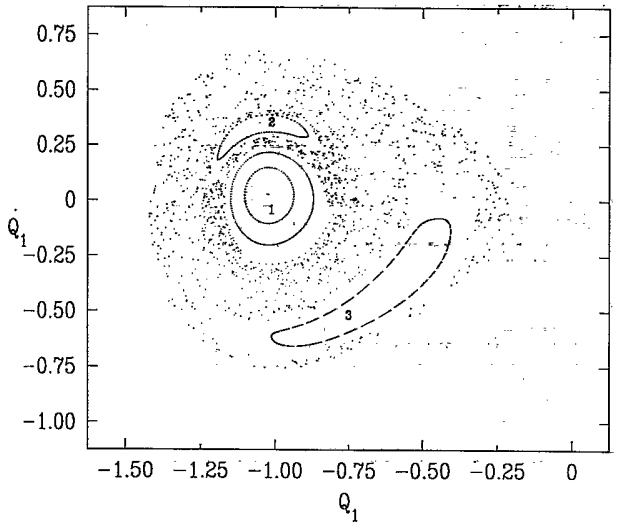

FIG. 6. Poincaré intersection between the trajectory and the subspace $\{\dot{Q}_1, Q_1, Q_0 = -1, \dot{Q}_0 > 0\}$ for the symmetric reduced three-particle problem Φ^4, $C = 0.1$ (see text), and energy $E = 0.580\,315$.

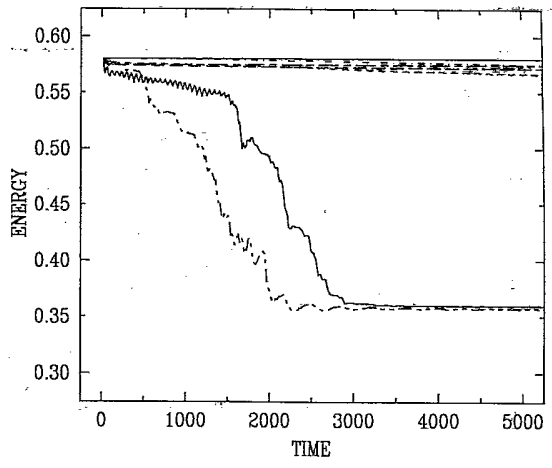

FIG. 7. $e_{(5)}(t)$ dependence for Φ^4, $C = 0.1$, and $N = 3000$. Long dashed line, initial condition from Fig. 2 (torus in island 2 in Fig. 6); short-long dashed line, fixed point in island 2 in Fig. 6; short dashed line, larger torus in island 1 in Fig. 6; dash-dotted line, fixed point in island 1 in Fig. 6; solid line, torus in island 3 in Fig. 6; long-short-short dashed line, chaotic trajectory in Fig. 6; and horizontal (highest) solid line, total energy of all simulations.

amplitude ratio does not indicate localization. Thus we expect a decay of those solutions in the full system. In Fig. 7 we see that these regular solutions of the reduced problem indeed decay in the full system. Finally we have to study the properties of the chaotic solutions. Since the amplitude ratios again do not indicate localization, we expect delocalized states in the full system. In Fig. 7 it is shown that the chaotic solutions indeed decay. But there is one puzzling detail—both the solution from island 3 and the chaotic solution decay in the full system until their energy comes to a value around 0.36; then we observe stabilization. No remarkable decay is observed for longer times. Certainly this energy value reflects some intrinsic property of our system. We will return to this problem later on and find the explanation.

Now we can formulate our correspondence conjecture. If we study NLE properties, we can define a reduced problem. The reduced problem will be not integrable. But it will have certain undestroyed regular orbits on tori in isolated subspaces (islands) of its phase space. Certain islands will correspond to NLE solutions in the full problem. An indication for that is the value of the amplitude ratio of the central and nearest-neighbor particles for trajectories from that island. Every trajectory from such an island of the reduced problem corresponds to a NLE solution of the full system. Since the trajectory evolves on a torus in the reduced problem, it generically leads to a multiple frequency NLE in the full system. The elliptic fixed points in such an island correspond to periodic (one-frequency) NLEs. They can be calculated using approximation techniques such as, e.g., RWA. Certain other islands of the reduced problem as well as the chaotic trajectories do not correspond to NLE solutions in the full system. They quickly decay because of energy radiation.

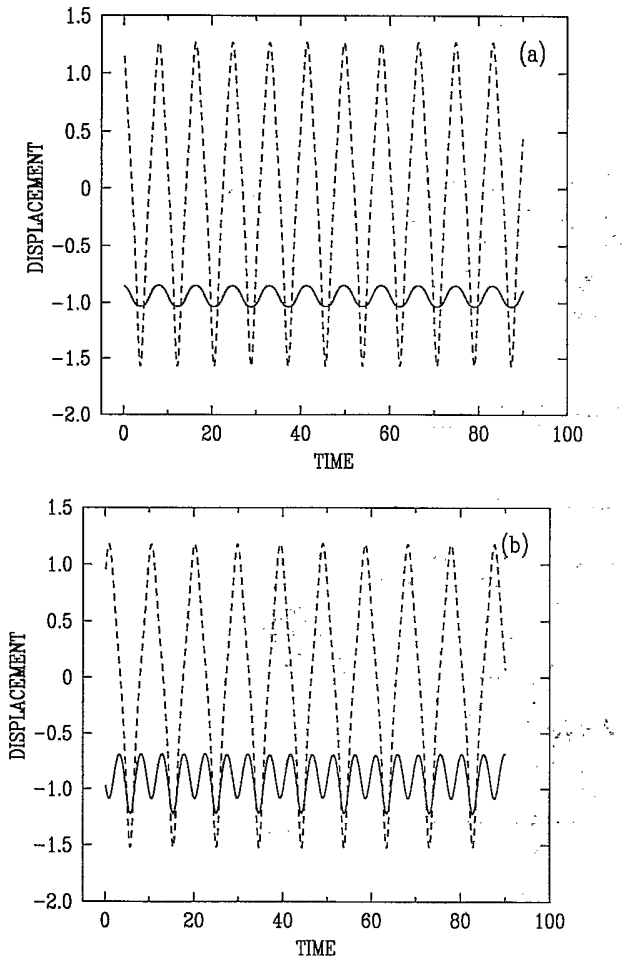

FIG. 8. Displacement of central (dashed line) and nearest-neighbor (solid line) particles versus time for Φ^4, $C = 0.1$, and $N = 3000$ with initial conditions corresponding to (a) fixed point in island 1 in Fig. 6 and (b) fixed point in island 2 in Fig. 6. Note that the measurement is performed after a waiting period of $t = 1000$.

C. NLE properties

To study properties of NLEs we first analyze the Poincaré map for the reduced problem with symmetric initial conditions over a large energy range. For small energies $E < 0.35$ we find no chaotic trajectories, so that nearly the whole reachable phase space consists out of regular trajectories [Fig. 9(a) for $E = 0.3$]. Near the "stochasticity" threshold $E_s = 0.35$ a (still small) fraction of chaotic trajectories is observed [Fig. 9(b) for $E = 0.35$]. The threshold value $E_s = 0.35$ is close to the depth of the ground state minimum of the potential describing Eqs. (21) and (22). In Fig. 9(c) we show the potential energy contour plot of (21) and (22). An analysis of the extrema yields four minima 1–4, a maximum 5, and several saddle points [cf. Fig. 9(c)]. The saddle point with the lowest energy $E = 0.38$ is point 6. The ground state is given by minimum 1. Increasing the energy starting with 1, one first hits the saddle point 6. Since there is a separatrix running through point 6 and tori are most likely destroyed near such separatrices, the appearance of the stochasticity threshold around $E = 0.35$ becomes understandable. Above the stochasticity threshold $E_s \approx 0.35$ the regular regions are separated into isolated islands. Between these islands chaotic motion occurs (cf. Fig. 6). At the same time we observe bifurcation effects, i.e., period doubling. The corresponding tori are multiple folded. At energies around 0.4 no regular islands are found—all trajectories seem to be chaotic. Around energies of 0.5 we again find regular islands. Finally around energies of 2.2 the character of the periodic orbits (fixed points in the Poincaré map) changes from in phase motion of the central and nearest-neighbor particles to out of phase motion. The above discussion does not imply the nonexistence of chaotic motion below the stochasticity threshold. It is the observable fraction of chaotic trajectories that we refer to.

As we have shown, certain regular islands of the Poincaré map of the reduced problem yield NLEs in the full system. The properties of those solutions can be characterized by analyzing the corresponding periodic orbits (fixed points in the map). Especially the stability of the many frequency solutions in the full system will depend on the stability of the periodic orbits. Thus we determine the periodic orbits for different energies $E \leq 3$. The fundamental frequency ω_1 is shown in Fig. 10 (triangles) as a function of the energy. Next we simulate the

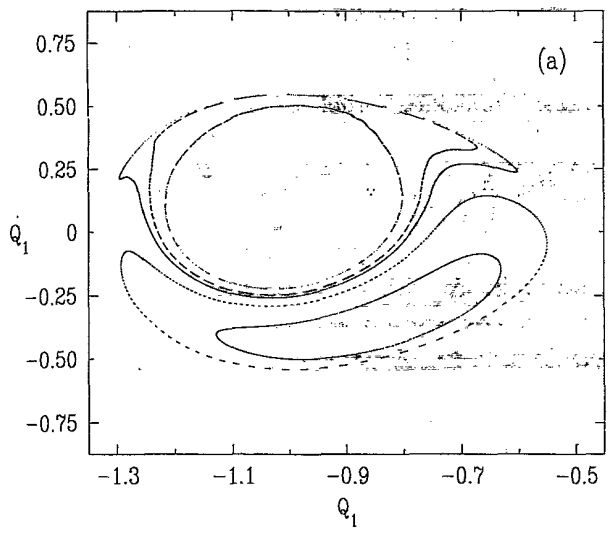

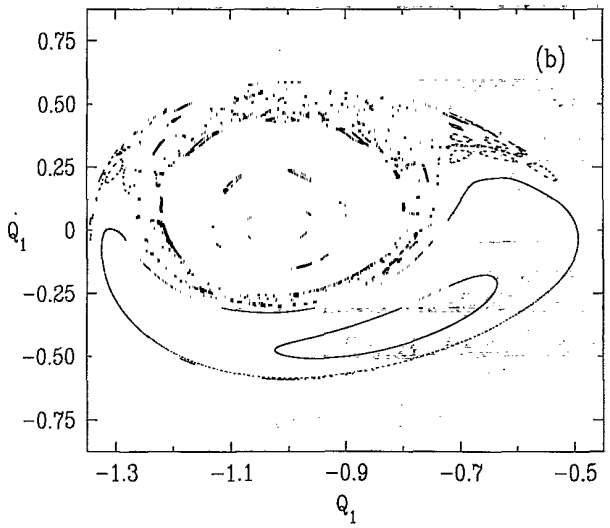

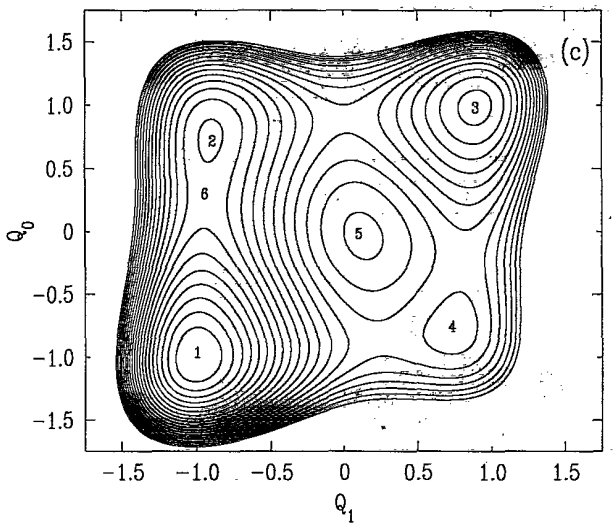

FIG. 9. (a) Same as in Fig. 6 but for $E = 0.3$; (b) same as in Fig. 6 but for $E = 0.35$; (c) contour plot for the potential energy of the reduced Φ^4 problem. Lines are drawn in energy distances of $E = 0.05$ starting with the ground state $E = 0$.

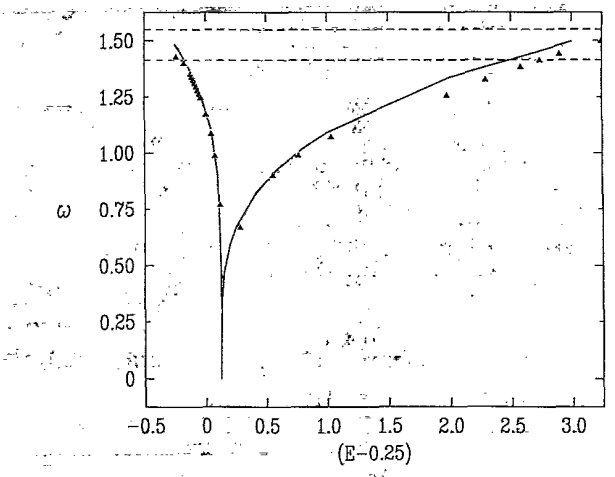

FIG. 10. Fundamental frequency of oscillation of a particle in the effective potential (26) versus energy (solid line). Triangles, fundamental frequency of the fixed points of the reduced Φ^4 problem versus energy; dashed lines, band edges of the phonon band.

full system with initial conditions that correspond to the periodic orbits of the reduced problem. We then monitor the energy distribution $e_l(t)$ over 10 000 time units. We find that below a certain energy threshold $E_c \approx 0.1$ no stationary NLEs can be created; instead the energy is quickly transported out of the excitation region. Above the mentioned threshold long-lived NLEs are observed. To characterize the energy distribution, we calculate a normalized entropy σ:

$$\sigma = -\frac{1}{\ln N} \sum_l p_l \ln p_l, \tag{24}$$

where $p_l = e_l / \sum_l e_l$. From the definition we have $0 < \sigma < 1$. Delocalization occurs if $\sigma = 1$ and maximum localization if $\sigma = 0$ [17]. In Fig. 11 the dependence of σ on the initial energy and the NLE energy (if it exists)

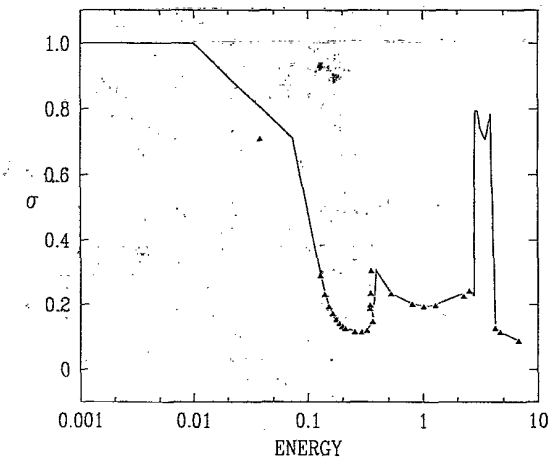

FIG. 11. Normalized entropy σ for Φ^4, $C = 0.1$, $N = 3000$ and initial conditions corresponding to the fixed point solutions of the reduced problem. Solid line, versus initial energy; triangles, versus NLE energy.

is shown. The mentioned energy threshold $E_c \approx 0.1$ is clearly seen. Note that around the stochasticity threshold $E_s \approx 0.36$ of the reduced problem $\sigma(E)$ has a step. Also at higher energies $E \sim 2$–4 an instability occurs again. This instability is due to a coupling of NLEs to small amplitude phonons (see Sec. V).

D. Approximation scheme

Now that we have shown that the NLE we are dealing with are a result of local (quasi-)integrability of the system under consideration, we want to discuss an approximation scheme to account for the basic features of the NLE.

In the continuum limit one can try to solve the corresponding partial differential equations. That was done in numerous publications. The other logical limit is when the amplitude of oscillation of neighbor particles differs strongly, i.e., $|Q_{l-1} - \eta|^{\max} \gg |Q_l - \eta|^{\max} \gg |Q_{l+1} - \eta|^{\max}$, $l \geq 1$. Surprisingly this condition does not restrict the system to the order-disorder limit. The above discussed numerical results already fit into this condition, although we are dealing with an intermediate interaction. We now carry out an approximation scheme to account for frequencies and existence regions.

Let us assume that we are dealing with a NLE such that $|Q_0 - \eta|^{\max} \gg |Q_{\pm 1} - \eta|^{\max}$. Then a starting point could be to consider the equation of motion for the central particle neglecting the small-amplitude fluctuations of the nearest neighbors. We arrive at the effective one-particle problem

$$\ddot{Q}_0 = -\frac{dV_{\text{eff}}}{dQ_0} \quad , \tag{25}$$

where the effective potential V_{eff} is given by the expression

$$V_{\text{eff}}(x) = V(x) + C(x - \eta)^2 \quad . \tag{26}$$

Using the amplitude of the central particle as an input parameter, one can solve Eqs. (25) and (26) with respect to the fundamental frequency ω_1. The result is shown in Fig. 10 (solid line). We find remarkable coincidence with the frequency versus energy dependence of the regular orbits of the reduced problem (triangles).

To account for the second frequency let us consider the equation of motion for the nearest neighbor Q_1 using $|Q_1 - \eta|^{\max} \gg |Q_2 - \eta|^{\max}$:

$$\delta\ddot{Q}_1 = -\left.\frac{dV}{dQ_1}\right|_{Q_1 = \eta + \delta Q_1} - 2C\delta Q_1 + CQ_0 \quad . \tag{27}$$

This equation describes a driven nonlinear oscillator, where CQ_0 is the driving term. If the amplitude of the nearest neighbor is small enough, the nonlinearity coming from $V(Q_1)$ can be approximately handled by replacing the original anharmonic potential by a harmonic one with amplitude-dependent frequency. Nevertheless we are still confronted with a complicated problem, since the driving term is not a harmonic function. But we have seen in Sec. III that neglecting the higher harmonics for the motion of a particle in a nonlinear potential can be a rather good approximation. Thus finally assuming that the driving term in (27) is a harmonic function with frequency ω_1, we are able to solve the equation of motion for Q_1. Using the full amplitude of the nearest neighbor as an input parameter, one can solve for the second frequency ω_2 [17].

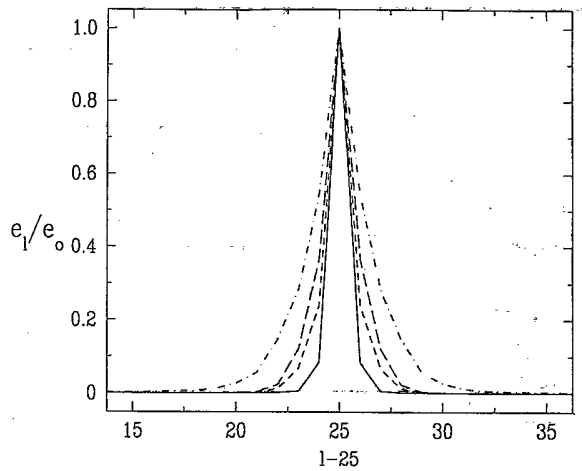

FIG. 12. Normalized energy distribution $e_l^{\max}/e_0^{\max}$ versus particle number for Φ^4, $N = 3000$. Solid line, $C = 0.1$, $E = 0.326$; short dashed line, $C = 0.3$, $E = 0.816$; long dashed line, $C = 0.5$, $E = 2.0$; dash-dotted line, $C = 1.0$, $E = 3.56$.

E. NLE shapes

In this subsection we want to briefly show our results with respect to the NLE shapes. For that we start a given simulation, wait a time period of 1000, and then perform a measurement during a time interval of 150. We measure the local energies and amplitudes for every particle independently and store their maximum values. These values as a function of the lattice site are then printed and can be viewed as (not normalized) distribution functions, especially in the case of the local energies. The values at each lattice site are, however, uncorrelated with respect to the time evolution, so that, e.g., the sum over the maximum local energy distribution function will not coincide with the real NLE energy (if it exists). Typical shapes for Φ^4 and $C = 0.1, 0.3, 0.5, 1.0$ are shown in Fig. 12. We see that a clearly defined NLE exists for different C values, and we observe that the width of the NLE increases as C increases. Note that we have not shown all results of simulations but only the typical ones with respect to the NLE. In fact we picked out the solutions with maximum localization property.

V. STABILITY ANALYSIS

In this section we will study several stability properties of NLE. First we analyze the stability of NLE with respect to small-amplitude phonons, which can be viewed as a realization of external (with respect to the NLE) parametric resonances. Then we show the existence of internal parametric resonances, i.e., the NLE becomes instable due to a transition from regular to chaotic mo-

tion. Finally we apply these results to the explanation of the existence of several energy thresholds.

A. External parametric resonance

Let us assume that we found an exact NLE solution $Q_l(t)$. To study the stability of such a solution with respect to small-amplitude oscillations (phonons) we consider a small deviation from this solution $Q_l(t) + \Delta_l(t)$, insert this ansatz in the original equations of motion, and linearize with respect to Δ. Finally we transform the equations into q space and find

$$\ddot{\Delta}_q + \omega_q^2 \Delta_q + \sum_{q'} \Delta_{q'} \left(\frac{2\alpha_1}{N} Q_{q-q'} + \frac{3\alpha_2}{N^2} \sum_{q''} Q_{q''} Q_{q-q'-q''} + \cdots \right) = 0 \ , \tag{28}$$

where the constants α_i are defined through the derivatives of the potential at the ground state position (numbers unimportant here). Unfortunately we are not able to make statements about the stability of waves in (28) if the NLE is described by more than one fundamental frequency. However, it is possible to proceed for the fixed point solutions, i.e., the periodic orbits. We introduce a vector

$$\mathbf{\Delta} = \left(\Delta_{q_1}, \dot{\Delta}_{q_1}, \ldots, \Delta_{q_N}, \dot{\Delta}_{q_N} \right) \ . \tag{29}$$

Then we can rewrite (28):

$$\dot{\mathbf{\Delta}} = \underline{M}(\{Q_q(t)\}, \mathbf{\Delta}) \ . \tag{30}$$

The linear matrix $\underline{M}$ has several interesting properties. The trace of the matrix is zero. The matrix is also periodic in time with period $T_1 = 2\pi/\omega_1$. Let us introduce a mapping A:

$$A\mathbf{\Delta}(t) = \mathbf{\Delta}(t + T_1) \ . \tag{31}$$

Following Arnol'd [23], a solution $\mathbf{\Delta}(t)$ is stable (and periodic with T_1) if the mapping A is stable. The mapping A is linear and volume preserving and the necessary condition of stability of a solution of (30) becomes

$$|\mathrm{tr} A| < 2N \ . \tag{32}$$

Since $Q_l(t)$ is a localized solution, its transformed counterpart $Q_q(t)$ is finite for every q, whereas a wave solution would be N times larger. Thus the $1/N, 1/N^2, \ldots$ terms in (28) let the additive perturbation terms in the differential equations of (28) and (30) become very small for large enough N. Then it is possible to study the stability of the mapping A neglecting the perturbation. Since the mapping matrix in that case becomes block-diagonal, the sufficient condition of stability reduces to

$$\frac{\omega_q}{\omega_1} \neq \frac{n}{2} \ , \quad n = 0, 1, 2, \ldots \ . \tag{33}$$

This stability condition implies the existence of instability bands on the frequency axis of the NLE because of the finite dispersion. We show this result in Fig. 13, where the dividing line between stable and unstable regions is drawn in the parameter space $\{C/4\omega_0^2, \omega/\omega_0\}$ with ω_0 being the lower band edge frequency.

Now it becomes clear why we find a threshold energy in the creation of NLEs (cf. Fig. 11). As is seen in Fig. 10, for small amplitudes (energies) the frequency of the periodic orbit is in the phonon band and thus the external parametric resonance sets in. The same happens for higher energies, where the frequency of the periodic orbits again crosses the phonon band. As expected, we do not find NLE solutions in the full system for these energies (cf. Fig. 11).

Although we cannot present analytical evidence for external parametric resonance in the case of many-frequency NLEs, we can make some rather obvious conjectures. If the NLE is described by a *finite* set of frequencies $\omega_1, \omega_2, \ldots, \omega_n$, generically there will always exist a set of integers $k_1, k_2, \ldots, k_n, k_q$ such that the expression

$$(k_1\omega_1 + k_2\omega_2 + \cdots + k_n\omega_n)/k_q \tag{34}$$

will be equal to a phonon frequency ω_q at least for a certain value of q. Then we would expect energy radiation because of parametric resonance. Our simulation results confirm that conjecture—for all many-frequency NLEs weak energy radiation is observed. Thus we come to the conclusion that many-frequency NLEs are, strictly speaking, unstable, although the time scale of their decay (lifetime) can be very large compared to the internal oscillation periods $2\pi/\omega_k$. However, if we let the phonon band width going to zero, then we expect these lifetimes to become infinite. Certainly this limiting case is trivial in the case of the discrete Klein-Gordon systems we consider in this work. But our stability analysis applies to *any* discrete system, assuming the existence of (many-frequency) NLEs and small-amplitude phonons. Thus we expect our limit of vanishing bandwidth to become

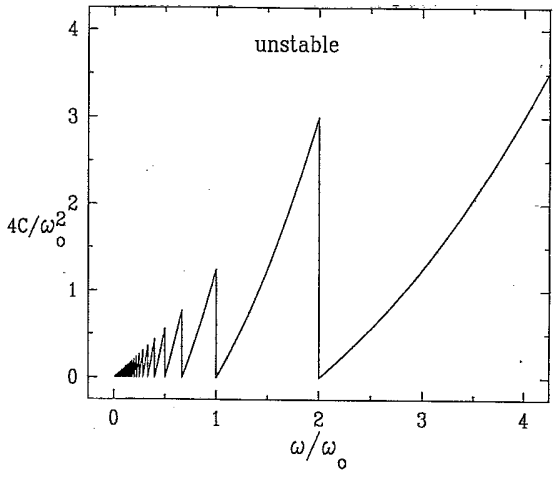

FIG. 13. Stability phase diagram of periodic NLEs.

relevant for other classes of systems as, e.g., the Fermi-Pasta-Ulam systems are.

B. Internal resonance

As mentioned in Sec. V A, there are no internal resonances for many-frequency NLEs in the generic case. But we remind the reader that we are dealing with nonlinear systems and we always have (at least weak) energy radiation of many-frequency NLEs because of external parametric resonance with phonons. Then the energy of the NLEs will adiabatically slowly decrease. Thus all parameters of the NLE (actions, frequencies) are also adiabatically slowly tuned. In the language of our Poincaré mappings this means that the trajectory drifts across the torus family for different energies. Looking at Fig. 6 we have three possibilities: (i) the trajectory drifts *towards the center* of the regular region to a periodic orbit—then we expect generically asymptotic stabilization of the NLE; (ii) the trajectory drifts *towards the boundary* of the regular region—then it comes close to a *resonant* torus defined by the vanishing of expression (34) for a certain set of integers $k_1, k_2, \ldots, k_n$; (iii) the trajectory stays somewhere in the regular region (no drift to center or boundary of the regular region)—then the energy radiation would continue until the NLE dissappears.

Possibility (iii) seems to be nongeneric, thus we are left with (i) and (ii). Case (ii) implies that because of the weak energy radiation of the many-frequency NLE it tunes itself towards an internal parametric resonance. What do we expect in that case? From the Kol'mogorov-Arnol'd-Moser (KAM) theorem (cf., e.g., [22]) we know that slightly perturbing an integrable system leads to stochastic motion in phase-space regions around certain resonant tori. Thus once our NLE hits the resonant condition (or in fact comes close enough to it) the internal dynamics of the particles becomes chaotic and aperiodic. That means that instead of discrete spectra we find continuous spectra for the Fourier transformed particle motion. That means that the overlap of nonzero parts of the spectrum with the phonon band dramatically increases leading to an *increased* energy radiation. Indeed in Fig. 14 (short dashed line) we see the time dependence of the NLE energy for the scenario as described above. We checked numerically that as the energy is radiated in the first part of the evolution, the frequencies ω_1 (decreases with time) and ω_2 (increases with time) are self-tuned towards a resonance $2\omega_1 = \omega_2$. At the time threshold $t \approx 6000$, where we observe an increase of the energy radiation per time of the order of 100, the spectra become continuous. The remaining puzzle is the following: Why are all unstable trajectories (NLEs with internal parametric resonances, other instable trajectories as seen in Fig. 7) stabilized, if the energy becomes lower than a threshold value of approximately 0.36? The answer seems to be the existence of a stochasticity threshold in the energy of the reduced problem (cf. Sec. IV C). Indeed, if the energy of the NLE becomes lower than the stochasticity threshold value of approximately 0.36, then the spectra have to become discrete again, thus the energy radiation can abruptly slow down (if the main frequencies ω_k do not overlap with the phonon band).

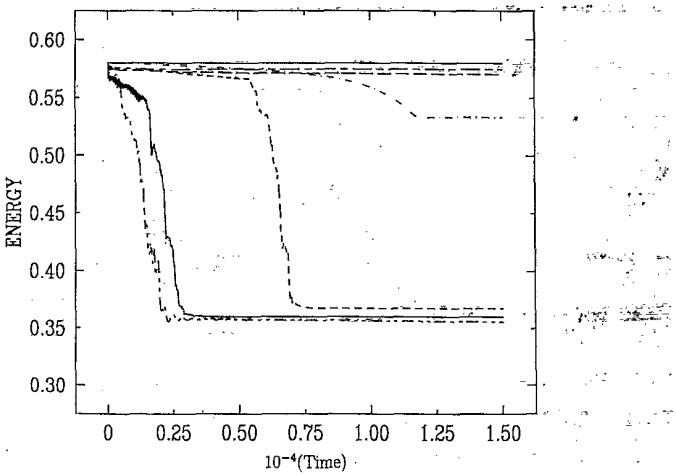

FIG. 14. Same as in Fig. 7 but longer time scale. Note the rapid decrease of $e_{(5)}$ as given by the short dashed line around $t = 6000$.

One comment should be added to explain the validity of the stability analysis. We have studied stability of assumed existing periodic (one-frequency) NLEs with respect to certain perturbations such as, e.g., phonons. A rigorous stability analysis implies much more effort and was outside of our initial purpose. As Campbell and Peyrard have shown [15], one has to find the periodic solution (NLE) on a large enough lattice and then to calculate the eigenvalues of the mapping A [cf. (31)] for any perturbation. Only if all eigenvalues are of modulus 1 can we conclude that the periodic NLE is stable. Indeed Campbell and Peyrard found for the Φ^4 system that the periodic NLE solutions (fixed points in the Poincaré mapping) are stable.

VI. OTHER KLEIN-GORDON SYSTEMS

A. Φ^3 system

This system is described by the potential (2). It is not very different from the Φ^4 system if one considers only one-well motions. Indeed we again find many-frequency stationary NLEs which can be described by a reduced problem. A representative Poincaré map is shown in Fig. 15 for energy 0.273 491 6 and $C = 0.1$. It is interesting to note that many-frequency NLEs were found in this system already in [16], where the authors have interpreted the additional peaks in the spectra as due to band edge phonons. The reason they attributed the corresponding peaks in the spectra to band edge phonons is that in the Φ^3 system the frequency ω_2 separates from the phonon band edge only for energies very close to the global instability of the model.

B. Double quadratic system

In that case the Hamiltonian is given in (4). The DQ system has to be considered as a very special case, probably the exception of the rule within the Klein-Gordon

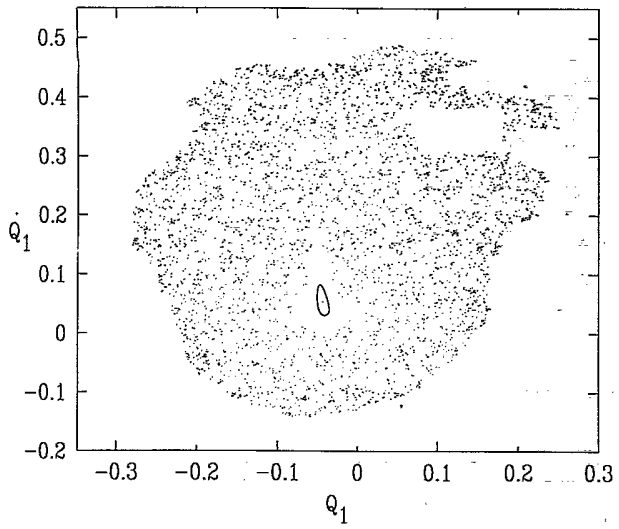

FIG. 15. Same as in Fig. 6 but for Φ^3.

class. Its kink properties, e.g., substantially differ from other Klein-Gordon kinks (cf. [24]). That holds also for the NLE properties. Let us apply our integrability conjecture. We construct the reduced problem and find that there should be again a threshold in the NLE energy. Below the threshold no NLEs are excitable. The threshold is simply defined by the fact that for amplitudes of the central particle to small to overcome the barrier the whole system behaves like a harmonic chain. However, the increase of the energy above that threshold allows the central particle to overcome the barrier. Then we expect a sudden drop of the frequency ω_1 into the gap (at least for small enough values of C), as it comes out of the effective potential construction. For large enough energies the frequency ω_1 will come into the band again and stay there for all higher energies. Since the frequency ω_2 can be connected with the motion of the nearest neighbors we expect those additional frequencies to stay always in the phonon band (because of the small amplitudes of the neighbors). That means that we always have resonance

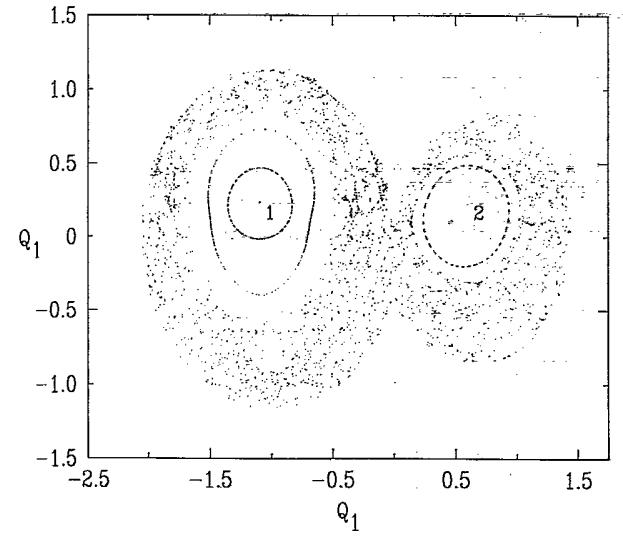

FIG. 16. Same as in Fig. 6 but for double quadratic model.

of the additional frequencies with the phonons. Thus the energy stored in the additional degrees of freedom of the NLE should be radiated away. Then we are left with a periodic orbit (fixpoint solution). In Fig. 16 we show the Poincaré map of the reduced problem for an energy above the threshold $E = 1.4$ ($C = 0.1$). We observe regular islands separated by chaotic trajectories. Such phase space structures were found for similar piecewise parabolic potentials by Kob and Schilling [25]. Regular region 1 in Fig. 16 corresponds to localization of energy. However, in the full system all initial conditions from this regular region collapse onto a periodic orbit with smaller energy (still above the threshold value). In other words, we find only one-frequency stationary NLEs in the full system. It reminds us of the properties of attractors in nonconservative systems [22].

VII. DISCUSSION

As our study shows, it is possible to describe very localized oscillating excitations on a discrete lattice. The method consists of constructing a reduced problem of a few degrees of freedom and analyzing its phase-space structure with the help of geometrical methods (Poincaré mappings). We have shown that it is possible to find a correspondence between certain regular regions of the reduced problem and long-lived localized excitations on an infinite lattice. Furthermore we have carried out the stability analysis of the elliptic fixed points of the regular islands with respect to small-amplitude phonons. Since the elliptic fixed points are always inside the regular regions, one also can expect from that result generic statements about NLEs which correspond to motion on tori surrounding the elliptic fixed point solutions. Naturally the NLEs corresponding to motion on tori are characterized by more than one frequency. We followed the evolution of the energy distribution in the infinite lattice and thus were able to express numerically the energy distribution within the NLE by means of a normalized entropy. As it follows from the stability analysis, generically multiple-frequency NLEs are always weakly radiating energy due to interaction with phonons. This leads to several interesting relaxation patterns. We find the existence of an energy threshold to create NLEs as well as a stochasticity (energy) threshold which separates completely regular phase space from isolated regular islands separated by a chaotic sea. All those values become important if one considers dynamic (relaxational) and thermodynamic properties of lattices with finite temperatures (energies per particle). Especially the existence of multiple frequency NLEs implies that the statistical weight of those excitations should be much larger than the statistical weight of the single-frequency NLEs (the elliptic fixed points in the Poincaré map).

All of the above statements were studied for different models belonging to the class of one-dimensional Klein-Gordon lattices. We found excellent agreements for our findings with numerical data. From our method it follows that no principal problems appear in higher dimensions. It is only a matter of constructing the correct reduced problem.

More difficulties could appear if one switches to model classes with total momentum conservation. At least for several FPU systems it is known that NLEs can move nearly freely [5]. Then we expect a geometrical misfit of the fact having many-frequency stationary NLEs and moving NLEs as we will show in a forthcoming paper. One could also pose the question whether in the Klein-Gordon class moving NLEs are possible. In the energy ranges considered in this contribution we never observed moving NLEs. However, it could be possible to excite moving NLEs at higher energies (cf. Fig. 14 in [26]). The question "are they moving or not?" was considered by several groups [27, 28]. Essentially the idea was to take over the fruitful methods to derive Peierls-Nabarro potentials for moving kinks in discrete lattices. Those Peierls-Nabarro potentials are the result of the discretization of the corresponding PDE and cause self-pinning of kinks. In the continuum limit, i.e., going over from the CODE to the PDE, the Peierls-Nabarro potential vanishes and the continuous symmetry group is restored—the kinks can move freely, no pinning occurs. However, it is well known that very discrete oscillating NLEs can freely move through the integrable Ablowitz-Ladik lattice. As some numerical work indicates, their movability is destroyed by adding nonintegrable perturbations [27, 28]. But we would be careful in overestimating those *numerical* results. The FPU systems are believed to be nonintegrable, nevertheless moving NLEs seem to exist. Also it is not known what kind of symmetry a lattice needs in order to support moving NLEs. Certainly it seems to be too simple to use the discretization procedure to derive Peielrs-Nabarro potentials as it was done for kinks. Not only that, two of us have shown recently that, strictly speaking, there is no possibility to connect the CODE and PDE smoothly by means of perturbation methods [24]. One also has to remember that our oscillating NLEs have internal degrees of freedom which essentially characterize them. The coupling of these degrees of freedom to the lattice has to be taken into account.

Let us apply our method to some special discrete systems of the FPU type. First we discuss the FPU23 system, where the polynomial of the nearest-neighbor interaction potential is of third order. Constructing the effective potential in that case, we find the fundamental frequency being always in the acousticlike phonon band. Thus no NLE solutions are expected in this case. Indeed no such solutions were found in numerical experiments [29]. Another instructive case is the related Toda lattice with exponential nearest-neighbor interaction [12]. Again the fundamental frequency of the effective potential would be always in the phonon band, thus no NLEs are expected to exist. This is especially interesting because of the fact that the Toda lattice is completely integrable. Again numerical search failed to find NLEs [29, 30]. Finally let us consider a FPU lattice with pure quartic nearest-neighbor springs. In that case there exist no small-amplitude linear phonons. Thus we would conclude that NLEs can exist at *all* energies. Indeed Page [8] has confirmed the existence of a NLE for a certain energy. But because of the homogeneity of the potential energy in the particle coordinates it follows that a solution of the system at a certain energy will be also a solution of the system for any other energy provided that time and coordinates are scaled properly [31]. Since the coordinate scaling is homogenous, the localization character of the NLE solution as found by Page will be unchanged. These examples show how powerful our method is in forecasting properties of lattices with respect to NLE solutions.

Why is the whole issue of NLEs so interesting? Well, the main reason for the occurrence of NLE is the nonlinearity of the system, which expresses itself by an energy dependence of oscillation frequencies of the particles. The rest can be understood in analogy (although all analogies have their weaknesses) to a harmonic lattice with mass defects. The mass defects essentially lead to a variation of frequencies with lattice sites. That is enough to suppress energy exchange and to produce the well-known localization phenomena in those systems. Now nearly everywhere in modeling reality we are confronted with the necessity to consider nonlinear systems. If they are in addition discrete, then we would expect NLEs to appear at least under certain circumstances, but more or less independent of the system. The NLEs discussed in the present work are properties of certain integrable systems partially destroyed by the nonintegrable perturbations. In other words, there exists an intrinsic source for localization of vibrational energy in nearly every nonlinear lattice.

One can pose the question whether the NLE solutions can exist in lattices at finite temperatures (or energies per particle). So far our studies of the NLEs were done on infinitely small energies per particle considering the thermodynamic limit $N \to \infty$ and could be considered as a consequence of the KAM theorem implying that the energy per particle was smaller than the threshold above which essentially all regular tori are destroyed [22]. This threshold decreases exponentially with the number of particles ([32] and references therein). The improvement of KAM theory by Nekhoroshev [33, 34] deals with finite-time stability of regular orbits (instead of infinite-time stability as in the KAM theory) and also yields a threshold which quickly drops to zero in the thermodynamic limit [32]. Thus from this side we could expect our NLEs to vanish at finite temperatures in infinite lattices. However, the NLE solutions are localized, thus the energy density still remains finite at least at certain lattice sites. If we consider a lattice of densely packed NLEs and remember that the energy radiation and thus the NLE-NLE interaction can be very weak, the motion of the whole system close to regular orbits should be possible. In that case also the temperature would be finite. Finally, exactly because the NLEs can be very localized (on a few particles) the KAM and Nekhoroshev thresholds for every subsystem (cf. the discussed reduced problem) will be finite and large thus allowing us to expect NLEs in infinite lattices at rather high temperatures.

Previous simulations of discrete Klein-Gordon systems with Morse on-site potentials and of Φ^4 lattices at finite temperatures have shown the appearance of NLEs in high density (cf. Fig. 4 in [35] and Fig. 14 in [26], respectively). This fact is not a proof of our conjecture, but already two models where NLEs seem to be the proper

quasiparticles to describe the excitational spectrum as well as the relaxational properties of the model is exciting. There are attempts to understand the dynamical process of creation of NLEs [36]. It might be that underlying finite-time singularities of PDE are important [37], where one finds energy localization due to the presence of those singularities.

It is interesting to note that Birnir has recently shown that breathers in the sine-Gordon PDE are of isolated character, namely, they remain as solutions of the perturbed sine-Gordon PDE only under two isolated perturbations [38]. In the case of discrete lattices as studied in the present work we cannot find any evidence for an analogous isolated character of the NLE solutions. Moreover in our opinion the perturbations which destroy the NLE solutions are of the isolated type. Thus breatherlike oscillating NLEs seem to be very different from their continuum counterparts with respect to their applicability.

Finally we want to emphasize that the developed geometrical method to describe NLEs in discrete systems can be of use if one studies connections between different model classes as well as the continuum limit. That would shed light onto the connection between CODE and PDE.

We think that the localization effects considered in this paper can be of importance not only in one-dimensional classical Hamiltonian lattices. There are interesting questions concerning higher dimensions, quantum lattices, connections to glass-like behavior of monocrystals at low temperatures, phase transitions in discrete systems, heat transport, and certainly other topics where we expect NLEs can essentially contribute to the understanding of properties of nonlinear systems.

ACKNOWLEDGMENTS

We thank M. Peyrard, S. Takeno, B. Birnir, O. V. Usatenko, and A. Neuper for interesting discussions. This work was supported in part (S.F.) by the Deutsche Forschungsgemeinschaft (Grant No. Fl 200/1-1).

[1] A. C. Newell, *Solitons in Mathematics and Physics* (Society for Industrial and Applied Mathematics, Philadelphia, 1985).
[2] R. Boesch and M. Peyrard, Phys. Rev. B **43**, 8491 (1991).
[3] M. J. Ablowitz and J. F. Ladik, J. Math. Phys. **17**, 1011 (1976).
[4] A. J. Sievers and S. Takeno, Phys. Rev. Lett. **61**, 970 (1988).
[5] S. Takeno and K. Hori, J. Phys. Soc. Jpn. **60**, 947 (1991).
[6] S. Takeno, J. Phys. Soc. Jpn. **61**, 2821 (1992).
[7] S. R. Bickham, S. A. Kisilev, and A. J. Sievers, Phys. Rev. B **47**, 14 206 (1993).
[8] J. B. Page, Phys. Rev. B **41**, 7835 (1990).
[9] K. W. Sandusky, J. B. Page, and K. E. Schmidt, Phys. Rev. B **46**, 6161 (1992).
[10] *Proceedings of the NATO Advanced Research Workshop and Emil-Warburgh-Symposium on Nonlinear Coherent Structures in Physics and Biology, 1993, University Bayreuth*, edited by K. H. Spatschek and F. G. Mertens (Plenum Press, New York, 1993).
[11] J. Ford, Phys. Rep. **213**, 271 (1992).
[12] M. Toda, *Theory of Nonlinear Lattices* (Springer-Verlag, Berlin, 1989).
[13] Y. A. Kosevich, Phys. Lett. A **173**, 257 (1993).
[14] S. Takeno, K. Kisoda, and A. J. Sievers, Prog. Theor. Phys. Suppl. **94**, 242 (1988).
[15] D. K. Campbell and M. Peyrard, in *CHAOS—Soviet American Perspectives on Nonlinear Science*, edited by D. K. Campbell (American Institute of Physics, New York, 1990).
[16] T. Dauxois, M. Peyrard, and C. R. Willis, Physica D **57**, 267 (1992).
[17] S. Flach and C. R. Willis, Phys. Lett. A **181**, 232 (1993).
[18] S. Flach and C. R. Willis, in *Proceedings of the NATO Advanced Research Workshop and Emil-Warburg-Symposium on Nonlinear Coherent Structures in Physics and Biology, 1993, University Bayreuth* (Ref. [10]).
[19] H. Thomas, in *Local Properties at Phase Transitions*, Proceedings of the International School of Physics "Enrico Fermi," Course LIX, edited by K. A. Müller (North-Holland, Amsterdam, 1976).
[20] Y. Onodera, Prog. Theor. Phys. **44**, 1477 (1970).
[21] S. Flach, Z. Phys. B **82**, 419 (1991).
[22] E. A. Jackson, *Perspectives of Nonlinear Dynamics* (Cambridge University Press, Cambridge, 1989 and 1990), Vols. 1 and 2.
[23] V. I. Arnol'd, *Ordinary Differential Equations* (MIT Press, Cambridge, 1973).
[24] S. Flach and C. R. Willis, Phys. Rev. E **47**, 4447 (1993).
[25] W. Kob and R. Schilling, J. Phys. A **22**, L633 (1989).
[26] S. Flach and J. Siewert, Phys. Rev. B **47**, 14 910 (1993).
[27] D. Cai, A. R. Bishop, and N. Groenbech-Jensen (unpublished).
[28] C. Claude, Yu. S. Kivshar, O. Kluth, and K. H. Spatschek, Phys. Rev. B **47**, 14 228 (1993).
[29] S. Takeno (private communication).
[30] A. Neuper (private communication).
[31] L. D. Landau and E. M. Lifshitz, *Mechanics* (Pergamon Press, New York, 1976).
[32] M. Pettini, Phys. Rev. E **47**, 828 (1993).
[33] N. N. Nekhoroshev, Funct. Anal. Appl. **5**, 338 (1971).
[34] N. N. Nekhoroshev, Russ. Math. Surv. **32**, 1 (1977).
[35] T. Dauxois, M. Peyrard, and A. R. Bishop, Phys. Rev. E **47**, 684 (1993).
[36] T. Dauxois, M. Peyrard, and C. R. Willis (unpublished).
[37] S. K. Turitsyn, Phys. Rev. E **47**, R13 (1993).
[38] B. Birnir (unpublished).